Inorg. Chem. **2005**, *44*, 8794–8803

Cadmium(II), Nickel(II), and Zinc(II) Complexes of Vacataporphyrin: A Variable Annulene Conformation inside a Standard Porphyrin Frame

Ewa Pacholska-Dudziak, Janusz Skonieczny, Miłosz Pawlicki, Ludmiła Szterenberg, and Lechosław Latos-Grażyński*

Department of Chemistry, University of Wrocław, 50 383 Wrocław, Poland

Received July 11, 2005

5,10,15,20-Tetraaryl-21-vacataporphyrin, **1** (butadieneporphyrin, annulene–porphyrin hybrid), which contains a vacant space instead of heteroatomic bridge, gives diamagnetic zinc(II) **1**-ZnCl and cadmium(II) **1**-CdCl and paramagnetic nickel(II) **1**-NiCl complexes. A metal ion is bound in the macrocyclic cavity by three pyrrolic nitrogens. Coordination imposes a steric constraint on the geometry of the ligand and leads to two stereoisomers with a butadiene fragment oriented toward **1**-MCl-i or outward **1**-MCl-o of the macrocyclic center. **1**-CdCl-o, **1**-ZnCl-o, and the free base share a common ^{1}H NMR spectral pattern as the basic structural features of **1** are preserved after metal ion insertion. The ^{1}H NMR spectra of **1**-CdCl-i and **1**-ZnCl-i reflect a decrease of aromaticity accounted for by the inverted butadiene geometry. The proximity of the butadiene fragment to the metal ion induces direct couplings between the spin-active nucleus of the metal ($^{111/113}$Cd) and the adjacent ^{1}H nuclei of butadiene. The pattern of chemical shifts detected for isomeric **1**-NiCl-i and **1**-NiCl-o is typical for high-spin nickel(II) complexes of porphyrin analogues. Resonances 2,3-H of **1**-NiCl-o or **1**-NiCl-i present the chemical shift typical for the β-H pyrrolic position despite the vacancy in the location of nitrogen-21. Coordination of imidazole, methanol-d_4, acetonitrile-d_3, or chloride converts **1**-NiCl-i and **1**-NiCl-o into distinct species which contain two axial ligands: **1**-Ni(Im)$_2^+$; **1**-Ni(CD$_3$OD)$_2^+$; **1**-Ni(CD$_3$CN)$_2^+$; **1**-Ni(Cl)$_2^-$. The density functional theory (DFT) has been applied to model the molecular and electronic structure of feasible **1**-CdCl stereoisomers. The total energies calculated using the B3LYP/LANL2DZ approach demonstrate a very small energy difference (2.3 kcal/mol) between **1**-CdCl-o and **1**-CdCl-i stereoisomers consistent with their concurrent formation.

Introduction

An aza-deficient porphyrin 5,10,15,20-tetraaryl-21-vacataporphyrin, **1** (Chart 1), is an annulene−porphyrin hybrid and at the same time is directly related to 21-heteroporphyrins but has a vacant space instead of heteroatomic bridge.[1] In analogy to carbaporphyrinoids, to make a point about the nature of the pyrrole-replacing moiety, the name butadieneporphyrin can be coined for **1**. Significantly, this molecule preserves the fundamental structural and spectroscopic features of parental tetraarylporphyrin with three nitrogen atoms favorably prearranged for coordination.[1] In principle vacataporphyrin, named also [18]triphyrin(6,1,1), according to the nomenclature suggested by Franck and Nonn,[2] can be considered as a prototype of the subclass of modified porphyrins which are distinguished by the fact that they contain only three pyrrole or pyrrole-like rings, linked by two *meso* sp^2 carbons to form the tripyrrolic brace. Evidently this molecule is located on the crossroads of porphyrin and annulene chemistry.

Chart 1

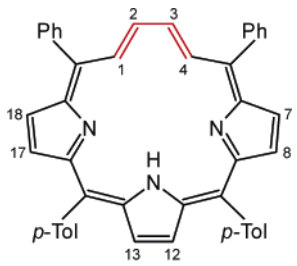

1

Formally, vacataporphyrin (butadieneporphyrin) can be formed from a porphyrin merely by extrusion of NH bridging

* To whom correspondence should be addressed. E-mail: LLG@wchuwr.chem.uni.wroc.pl.

(1) Pacholska, E.; Latos-Grażyński, L.; Ciunik, Z. *Chem.−Eur. J.* **2002**, *8*, 5403−5406.
(2) Franck, B.; Nonn, A. *Angew. Chem., Int. Ed. Engl.* **1995**, *34*, 1795.

10.1021/ic0511470 CCC: $30.25
Published on Web 10/18/2005

Chart 2

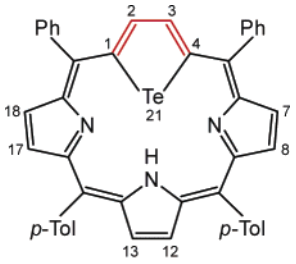

2

Chart 3

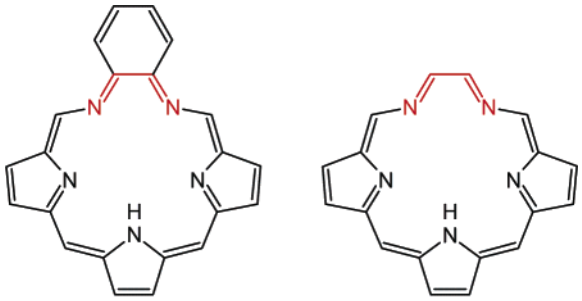

3 **4**

group followed by addition of two hydrogen atoms. Actually 5,20-diphenyl-10,15-bis(*p*-tolyl)-21-telluraporphyrin, **2** (Chart 2), was discovered to be a suitable precursor to form 5,20-diphenyl-10,15-bis(*p*-tolyl)-21-vacataporphyrin, **1**.[1]

Namely, extrusion of one heteroatom (Te), leading to vacataporphyrin **1**, gives an expanded coordination core, comparable by size and shape with texaphyrin **3**[3,4] (Chart 3) and related to theoretically investigated secophyrin **4**.[5] These molecules demonstrate a structural analogy to **1** provided that two CH groups of **1** have been replaced by two nitrogen atoms although the outer skeleton of the porphyrin remains unchanged.

It is significant to notice here that the macrocyclic delocalization pathway of vacataporphyrin **1**, which contains 18 π electrons, similarly as in the classical annulene model of porphyrin[6] is reminiscent of *p*-benziporphyrin **5 (**Chart 4).[7−10]

Modifications of a porphyrin coordination core lead to heteroporphyrins (including carbaporphyrins) which, in many cases, serve as macrocyclic ligands. If the heteroatom is bigger than nitrogen (S, Se, Te), the coordination core is contracted compared to a nonmodified porphyrin.[11] Carbaporphyrins, the recently explored class of macrocyclic

Chart 4

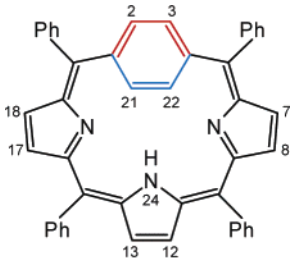

5

Chart 5

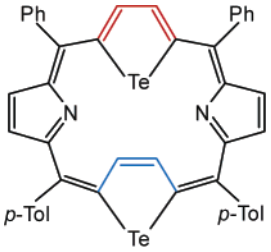

6

organometallic ligands, contain typically an inner C−H group exposed for coordination.[10−22]

The number of porphyrinoids with two linked carbon atoms in the macrocyclic core is very small, exemplified by *para*-benziporphyrin **5**[7,8] and 21,23-ditelluraporphyrin, **6** (Chart 5).[23] Evidently the annulene fragment of vacataporphyrin **1** is potentially exposed to coordination or interaction with coordinated metal ions to reveal the carbaporphyrinoid nature of **1**. Until the present coordination chemistry of vacataporphyrin escaped any experimental investigations which remains in contrast to widely explored texaphyrins.[24−26] Texaphyrin acts as a pentadentate ligand, which coordinates by three pyrrolic and two skeleton nitrogen atoms. In the

(3) Sessler, J. L.; Murai, T.; Lynch, V.; Cyr, M. *J. Am. Chem. Soc.* **1988**, *110*, 5586.
(4) Hannah, S.; Lynch, V. M.; Gerasimchuk, N.; Magda, D.; Sessler, J. L. *Org. Lett.* **2001**, *3*, 3911.
(5) Waluk, J.; Michl, J. *J. Org. Chem.* **1991**, *56*, 2729.
(6) Vogel, E. *Pure Appl. Chem.* **1993**, *65*, 143.
(7) Stępień, M.; Latos-Grażyński, L. *J. Am. Chem. Soc.* **2002**, *124*, 3838−3839.
(8) Stępień, M.; Latos-Grażyński, L.; Szterenberg, L.; Panek, J.; Latajka, Z. *J. Am. Chem. Soc.* **2004**, *126*, 4566−4580.
(9) Stępień, M.; Latos-Grażyński, L.; Szterenberg, L. *Inorg. Chem.* **2004**, *43*, 6654−6662.
(10) Stępień, M.; Latos-Grażyński, L. *Acc. Chem. Res.* **2005**, *38*, 88.
(11) Latos-Grażyński, L. Core Modified Heteroanalogues of Porphyrins and Metalloporphyrins. In *The Porphyrin Handbook*; Kadish, K. M., Smith, K. M., Guilard, R., Eds.; Academic Press: New York, 2000; pp 361−416.
(12) Chmielewski, P. J.; Latos-Grażyński, L.; Rachlewicz, K.; Głowiak, T. *Angew. Chem., Int. Ed. Engl.* **1994**, *33*, 779.
(13) Stępień, M.; Latos-Grażyński, L.; Lash, T. D.; Szterenberg, L. *Inorg. Chem.* **2001**, *40*, 6892.
(14) Venkatraman, S.; Anand, V. G.; Pushpan, S. K.; Sankar, J.; Chandrashekar, T. K. *Chem. Commun.* **2002**, 462.
(15) Graham, S. R.; Ferrence, G. M.; Lash, T. D. *Chem. Commun.* **2002**, 894.
(16) Muckey, M. A.; Szczepura, L. F.; Ferrence, G. M.; Lash, T. D. *Inorg. Chem.* **2002**, *41*, 4840.
(17) Hung, C.-H.; Chang, F.-C.; Lin, C.-Y.; Rachlewicz, K.; Stępień, M.; Latos-Grażyński, L.; Lee, G.-H.; Peng, S.-M. *Inorg. Chem.* **2004**, *43*, 4120.
(18) Furuta, H.; Asano, T.; Ogawa, T. *J. Am. Chem. Soc.* **1994**, *116*, 767.
(19) Srinivasan, A.; Furuta, H. *Acc. Chem. Res.* **2005**, *38*, 10.
(20) Furuta, H.; Maeda, H.; Osuka, A. *Chem. Commun.* **2002**, 1795.
(21) Ghosh, A. *Angew. Chem., Int. Ed.* **2004**, *43*, 1918.
(22) Harvey, J. D.; Ziegler, C. J. *Coord. Chem. Rev.* **2003**, *247*, 1.
(23) Pacholska, E.; Latos-Grażyński, L.; Ciunik, Z. *Angew. Chem., Int. Ed.* **2001**, *40*, 4466.
(24) Sessler, J. L.; Hemmi, G.; Mody, T. D.; Murai, T.; Burrell, A.; Young, S. W. *Acc. Chem. Res.* **1994**, *27*, 43−50.
(25) Lisowski, J.; Sessler, J. L.; Lynch, V.; Mody, T. D. *J. Am. Chem. Soc.* **1995**, *117*, 2273.
(26) Hannah, S.; Lynch, V.; Guldi, D. M.; Gerasimchuk, N.; MacDonald, C. L. B.; Magda, D.; Sessler, J. L. *J. Am. Chem. Soc.* **2002**, *124*, 8416.

case of smaller metal ions the tridentate character of texaphyrin was demonstrated as the pyrrolic nitrogen were solely engaged in coordination.[26]

The relevant coordination chemistry of *p*-benziporphyrin **5** has been studied systematically to show that this ligand assists weak metal−arene interactions.[7−10] Consequently, metallobenziporphyrins can be thought of as macrocyclic derivatives of tripyrrin complexes.[27−35] A remarkable structural diversity of nickel(II) tripyrrin complexes has been recently reported by Bröring and co-workers.[33,35]

The first part of our study deals with the diamagnetic Zn(II) and Cd(II) complexes of vacataporphyrin. The experimental approach takes advantage of our previous finding[7] that the proximity of the metal ion and arene gives rise to observable ^{1}H−M and ^{13}C−M scalar couplings in the NMR spectra. Such couplings are usually classified as "through-space" or "nonbonding" because their magnitude cannot be rationalized in terms of the network of formal bonds in the molecule.[36,37] Here couplings with the spin-active nuclei of $^{111/113}$Cd are used to detect a unique metal−butadiene interaction. In a complementary investigation the metal−butadiene interaction in high-spin Ni(II) vacataporphyrin complexes has been probed using their paramagnetically shifted ^{1}H NMR spectra.

Results and Discussion

Synthesis. 5,20-Diphenyl-10,15-bis(*p*-tolyl)-21-vacataporphyrin, **1**, was synthesized as described previously.[1] 5,20-Diphenyl-10,15-bis(*p*-tolyl)-21-telluraporphyrin, **2**, was used as a porphyrin-like substrate.[38] The straightforward conversion of **2** to **1** requires an addition of hydrochloric acid at high-temperature conditions controlled by the solvent reflux temperature (1,2-dichlorobenzene). The slight modification of the procedure using the stepwise instead of one-step acid addition afforded the yield improvement (72% after chromatographic workup). The replacement of HCl by DCl produces deuterated derivatives **1**-d_x, where deuterium atoms are bound to C(1) and C(4) (formerly α-tellurophene carbon atoms). The accompanying replacement of β-H pyrrolic atoms by deuterium resulted from their acidic nature. Significantly for further applications, the degree of deuteration is not reproducible from one synthesis to another. Typically the procedure gave samples which were approximately 100% deuterated at the 1,4-butadiene positions but 0% at 12,13-pyrrolic positions as shown by ^{1}H NMR. The deuteration levels at 7,8,17,18-pyrrolic (82−12%) and 2,3-butadiene (87−21%) locations varied (the level of deuteration given in parentheses). We have also detected that the H−D exchange rates at 7,18 and H-8,17 positions differ significantly. Consequently the shorter reaction times, which afforded smaller level of overall deuteration, produced vacataporphyrin preferentially labeled at 7,18-positions. A set of selectively deuterated vacataporphyrins facilitated the assignments of paramagnetically shifted resonances of paramagnetic complexes.

Insertion of zinc(II) and cadmium(II) into **1** has been readily achieved by adding a chloroform solution of the free base to a solution of an appropriate salt, usually anhydrous chloride, in acetonitrile. Only coordination of nickel(II) required some prolonged boiling. Usually the red reaction mixture turns bright green immediately. In all cases yields are quantitative (see Experimental Section). The zinc(II) and cadmium(II) complexes are not stable in the presence of traces of any acid. The resulting complexes will be denoted **1**-CdCl, **1**-ZnCl, and **1**-NiCl. The macrocycle acts as a monoanionic ligand coordinating through the three nitrogen donors. To compensate the charge of the metal dication, one additional anion is required. The identities of formed compounds were confirmed by high-resolution mass spectrometry and NMR spectroscopy.

NMR Spectra of Diamagnetic Vacataporphyrin Complexes. Zn(II) and Cd(II) complexes of vacataporphyrin yield well-resolved ^{1}H NMR spectra (Figure 1, traces B and C), which have been used to determine their structure in solution and eventually to study the metal−butadiene interaction. For comparison the spectrum of the free base vacataporphyrin[1] presenting the complete assignments of all resonances has been included in Figure 1.

Resonance assignments have been made on the basis of relative intensities and 2D COSY and NOESY experiments.

Coordination of a metal ion by vacataporphyrin imposes a steric constraint on the geometry of the ligand. To account for the spectral characteristic of **1**-MCl (Figure 1), we have initially considered two dominating macrocyclic conformations. The structure of metal(II) *p*-benziporphyrin, **5**-MCl, provided the reasonable reference model for our considerations. In this case the coordinating environment of M(II) forms a trigonal bipyramid, with the N(24) atom, chloride, and C(21)−C(22) bond occupying the equatorial positions.[7,8]

As found in the structure of **5**-CdCl, the *p*-phenylene moiety is positioned at an angle to the macrocyclic plane. Formally the replacement of C(21)H−C(22)H or C(2)H−C(3)H fragments by two hydrogens leads to two stereoisomers of **1**-MCl with the C(2)−C(3) bond directed outward in **1**-MCl-o or inward in **1**-MCl-i of the macrocycle as shown in Chart 6. Both isomers have an effective C_s symmetry, with the mirror plane passing through the metal ion, chloride, and pyrrolic (N23) nitrogen. As a consequence, the ^{1}H NMR spectrum will contain three pyrrole resonances (7,18-H, 8,17-H, and 12,13-H) and two multiplets of butadiene resonances (1,4-H and 2,3-H). Nonequivalence of two macrocyclic sides will cause each aryl ring to have two

(27) Montforts, F.-P. *Angew. Chem., Int. Ed. Engl.* **1981**, *20*, 778.
(28) Montforts, F.-P.; Schwartz, U. M. *Liebigs Ann. Chem.* **1985**, 1228.
(29) Eichinger, D.; Falk, H. *Monatsh. Chem.* **1987**, *118*, 261.
(30) Jauma, A.; Farrera, J.-A.; Ribo, J. M. *Monatsh. Chem.* **1996**, *127*, 936.
(31) Khoury, R. G.; Senge, M. O.; Colchester, J. E.; Smith, K. M. *J. Chem. Soc., Dalton Trans.* **1996**, 3937.
(32) Rath, S. P.; Olmstead, M. M.; Latos-Grażyński, L.; Balch, A. L. *J. Am. Chem. Soc.* **2003**, *125*, 12678.
(33) Bröring, M.; Prikhodovski, S.; Brandt, C. D. *J. Chem. Soc., Dalton Trans.* **2002**, 4213.
(34) Bröring, M.; Brandt, C. D. *Chem. Commun.* **2003**, 2156−2157.
(35) Bröring, M.; Prikhodovski, S.; Brandt, C. D. *Inorg. Chim. Acta* **2004**, *357*, 1733.
(36) Hilton, J.; Sutcliffe, L. H. *Prog. NMR Spectrosc.* **1975**, *10*, 27.
(37) Contreras, R. H.; Facelli, J. C. *Annu. Rep. NMR Spectrosc.* **1993**, *27*, 255.
(38) Latos-Grażyński, L.; Pacholska, E.; Chmielewski, P. J.; Olmstead, M. M.; Balch, A. L. *Angew. Chem., Int. Ed. Engl.* **1995**, *34*, 2252.

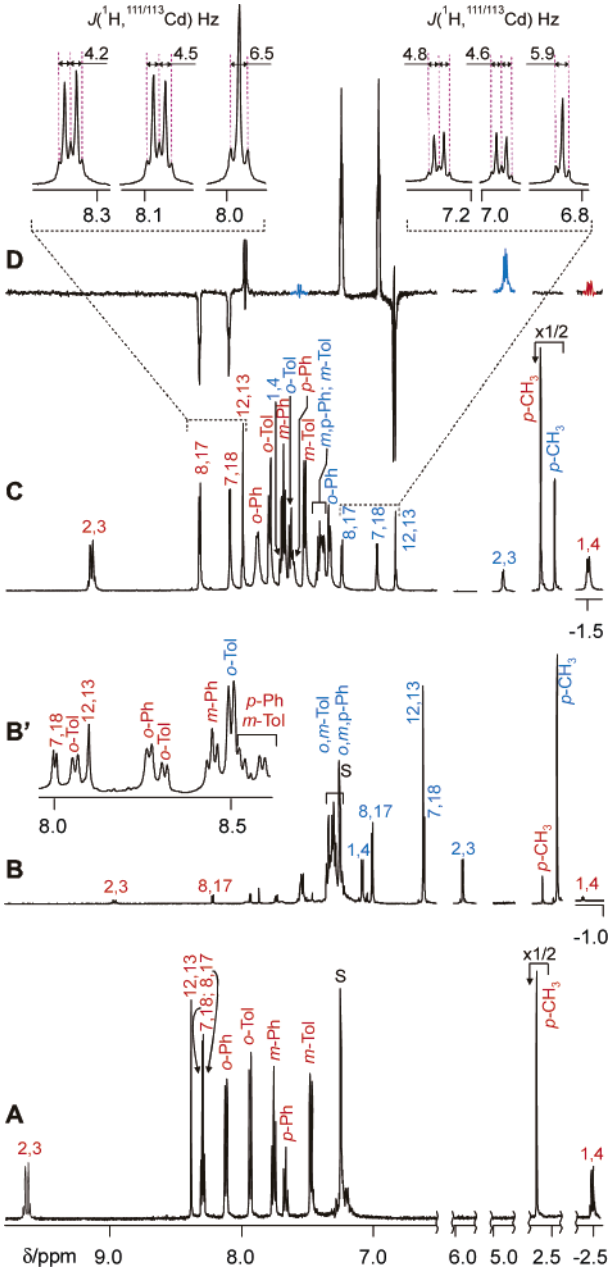

Figure 1. ^{1}H NMR spectra of (A) **1** ($CDCl_3$, 298 K) and (B) **1**-ZnCl ($CDCl_3$, 298 K). Inset (B′) presents the differentiation of *ortho* and *meta* resonances of **1**-ZnCl-o because of the slow rotation with respect to the $C_{meso}-C_{phenyl}$ at 230 K. The faster rotation at 298 K yielded broad lines. Also shown are (C) **1**-CdCl (CD_3CN, 298 K) and (D) 1D gsHSQC spectrum of **1**-CdCl (CD_2Cl_2, 298 K) showing the pattern of ^{113}Cd satellites due to weak cadmium−butadiene interactions (for **1**-CdCl-o in red; for **1**-CdCl-i in blue). The insets in (D) enlarge the ^{1}H NMR β-pyrrole resonances with cadmium satellites. Resonance assignments follow the numbering given in Chart 1 (**1**-MCl-o in red; **1**-MCl-i in blue).

distinct *ortho* and two *meta* resonances, unless the rotation around $C_{meso}-C_{ipso}$ bond is sufficiently fast.

Actually the ^{1}H NMR spectrum of **1**-CdCl (Figure 1, trace C) contains two complete sets of resonances readily assigned to two isomeric forms **1**-CdCl-o and **1**-CdCl-i exploiting the fact that the isomer **1**-CdCl-o, which shares a common ^{1}H NMR spectral pattern with the free base **1** (Figure 1, trace A), was more abundant in the analyzed sample. The concentration ratio [**1**-CdCl-o]/[**1**-CdCl-i] varies, however, for each preparation. Apparently, the composition of **1**-CdCl does not exhibit any temperature dependence indicating that the two isomers are not in fast dynamic equilibrium. The ratio [**1**-CdCl-o]/[**1**-CdCl-i] was monitored by NMR changes slowly in a chloroform solution. This final (o/i) ratio reaches 2:5 when the sample is stored in dark for 1 day at room temperature and 6:1 when exposed to daylight.[39]

A similar spectroscopic pattern has been detected for **1**-ZnCl (Figure 1, trace B) reflecting the presence of isomers **1**-ZnCl-o and **1**-ZnCl-i, but in this system the isomer **1**-ZnCl-i is preferentially formed. The isomers of **1**-CdCl (**1**-ZnCl) are inseparable by chromatography and crystallization. Actually, chromatography on alumina or silicagel resulted in demetalation.

1-CdCl-o, **1**-ZnCl-o, and the free base **1** have alike ^{1}H NMR spectral patterns which suggested that the basic structural features of **1** are preserved after metal ion insertion. The components of the AA′XX′ spin system assigned H1, H2, H3, and H4 of **1**-Cd-o, **1**-Zn-o, or **1** are located in downfield and upfield regions of the spectrum (Table 1, Figure 1). These shifts are consistent with the aromatic structure accepting a ring current effect as a criterion. Actually the AA′XX′ multiplets serve as the fingerprint of the annulene-like moiety (C1−C2−C3−C4). Remarkably, the ^{1}H NMR parameters of this pattern match those of [18]-annulene.[40,41] On the other hand, the ^{1}H NMR spectrum of the pyrrolic part of **1**-MCl-o exhibits typical for tetraaryl-21-heteroporphyrins values of J and δ.[11] The $\delta_{H2} - \delta_{H1}$ chemical shift differences equal 12.15, 10.77, and 9.28 ppm for **1**, **1**-CdCl-o, and **1**-ZnCl-o, respectively. The weakened aromatic current suggests some nonplanarity of the coordinated vacataporphyrin.

The ^{1}H NMR spectra of **1**-CdCl-i and **1**-ZnCl-i differ markedly from these measured for their **1**-CdCl-o and **1**-ZnCl-o counterparts**.** Thus, we have found that the coordination of cadmium(II) to yield **1**-CdCl-i affords a profound structural transformation of vacataporphyrin which involves a flip of the butadiene moiety and relocates the C(2)−C(3) unit from the periphery into the center of the macrocycle (Chart 6). The notable spectroscopic features of **1**-CdCl-i, revealing an unusual conformational flexibility of the vacataporphyrin macrocycle, include a spectacular downfield/upfield relocation of 1,4-H (−1.50 → 7.57 ppm) and 2,3-H (9.27 → 4.88 ppm) resonances when compared to isomeric **1**-CdCl-o. Similar chemical shift changes have been noticed for the **1**-ZnCl-o−**1**-ZnCl-i couple: 1,4-H (−0.32 → 7.07 ppm); 2,3-H (8.96 → 5.91 ppm).

The diagnostic shift difference between the outer and inner resonances of **1**-CdCl-o and **1**-ZnCl-o reflects their location in the deshielding (2,3-H) and shielding (1,4-H) zones of the diatropic ring current. The relatively modest ring current effect is still visible in the ^{1}H NMR spectra of **1**-CdCl-i and **1**-ZnCl-i. Here, the ring current contributions to 1,4-H and 2,3-H chemical shifts are in opposite direction as compared

(39) This photochemical isomerization is currently under investigation.
(40) Oth, J. F. M.; Bauman, H.; Gilles, J. M.; Schröder, G. *J. Am. Chem. Soc.* **1972**, *94*, 3498.
(41) Stevenson, C. D.; Kurth, T. L. *J. Am. Chem. Soc.* **2000**, *122*, 722.

Chart 6. Two Stereoisomers of 1-MCl Compared with *p*-benziporphyrin Complex **5**-MCl.

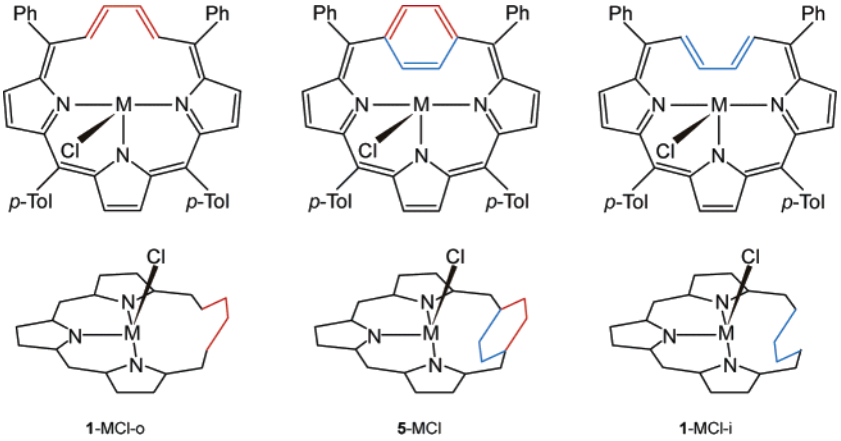

Table 1. ^{1}H NMR Data for **1**, **1**-CdCl, and **1**-ZnCl

compd	1,4-butadiene	2,3-butadiene	8,17-pyrrole	7,18-pyrrole	12,13-pyrrole
1[a]	−2.50	9.65	8.29	8.31	8.38
1-CdCl-o	−1.50	9.27	8.37	8.13	8.00
1-CdCl-i	7.57	4.88	7.23	6.94	6.82
1-ZnCl-o	−0.32	8.96	8.21	7.92	7.86
1-ZnCl-i	7.07	5.91	6.99	6.59	6.60

[a] Reference 1.

to **1**-CdCl-o and **1**-ZnCl-o, revealing the profound structural rearrangement.

The pyrrolic part of the **1**-CdCl-i (**1**-ZnCl-i) spectrum is placed in the relatively upfield region 6.82−7.23 (6.59−6.99) ppm, distinct from 8 to 8.37 (7.86−8.21) of **1**-CdCl-o (**1**-ZnCl-o) and is upfield shifted as compared to the free ligand (8.30−8.39 ppm).[1] The β-H chemical shifts **1**-CdCl-i and **1**-ZnCl-i resemble these of carbaporphyrinoids characterized by a relatively small degree of aromaticity.[42−45] Thus, **1**-CdCl-i and **1**-ZnCl-i exemplify the borderline cases of porphyrinoid aromaticity. Actually the small shift differences in the butadiene fragments for **1**-CdCl-i ($\delta_{H1} - \delta_{H2} = 2.69$ ppm) and **1**-ZnCl-i ($\delta_{H1} - \delta_{H2} = 1.16$ ppm) reflect the weak aromatic current and suggests marked nonplanarity of this macrocycle.

The highly nonplanar structure of **1**-MCl-i with an inverted conformation of the annulene fragment has the precedence in 21,23-ditelluraporphyrin **6**, where the diagnostic shifts of the β-tellurophene protons at 8.53 and 6.08 ppm were assigned to the regular and inverted rings, respectively.[23] The aromatic ring current effect of **6** is small because of the severe distortion, as reflected here by the difference in tellurophene chemical shifts, which equals 2.45 ppm.

The proximity of the butadiene fragment to the metal ion induces direct scalar couplings between the spin-active nucleus of the metal ($^{111/113}$Cd) and the adjacent ^{1}H nuclei. These couplings generate characteristic satellite patterns, which can be extracted from the 1D spectrum using appropriate filtering techniques (Figure 1, trace D). β-Pyrrolic protons **1**-CdCl-i and **1**-CdCl-o exhibit the usual four-bond couplings also known for regular cadmium(II) porphyrins[46] and cadmium(II) benziporphyrins.[7,8] In particular the inset in trace D of Figure 1 shows the 12,13-H multiplet patterns displayed by **1**-CdCl-o and **1**-CdCl-i, where the central line, which corresponds to the molecules containing spin-inactive Cd isotopes, is flanked with a pair of satellites. Significantly, the $^{111/113}$Cd satellites are detected for 1,4-H ($J_{H-Cd} \approx 7$ Hz) and 2,3-H ($J_{H-Cd} \approx 8$ Hz) of **1**-CdCl-i. A coupling is observed between $^{111/113}$Cd and protons 1,4-H ($J_{H-Cd} \approx 3$ Hz) of **1**-CdCl-o and, contrary to **1**-CdCl-i, is absent for 2,3-H. These couplings are too effective to be of the usual "through bond" origin because the metal nucleus and the proton are in five (1,4-H) or six (2,3-H) bonds apart and the geometry of the bond path is unfavorable. These couplings are therefore a result of the weak cadmium−CH "through space" interaction. In structural terms the detected coupling reflects the spatial proximity between the cadmium ion and the butadiene fragment, which differ in **1**-CdCl-o and **1**-CdCl-i. The side-on location of cadmium(II) with respect to the butadiene fragment in the folded structure of **1**-CdCl-i affords the simultaneous contacts with all C−H and C−C units of butadiene. Contrary, the 2,3-H hydrogens, located at the perimeter of the extended planar structure of **1**-CdCl-o, avoid any "through space" interaction.

NMR Spectra of Paramagnetic Chloronickel(II) Vacataporphyrin. Owing to the nonplanar coordination geometry of the metal ion, the nickel(II) complex of vacataporphyrin **1**-NiCl is paramagnetic, with $S = 1$. Similarly as described for diamagnetic **1**-CdCl and **1**-ZnCl complexes, **1**-NiCl is actually a mixture of two conformers: **1**-NiCl-o and **1**-NiCl-i presented in Chart 6. The specific assignment

(42) Chmielewski, P. J.; Latos-Grażyński, L. *J. Chem. Soc., Perkin Trans. 2* **1995**, 503.
(43) Chmielewski, P. J.; Latos-Grażyński, L.; Głowiak, T. *J. Am. Chem. Soc.* **1996**, *118*, 5690.
(44) Sprutta, N.; Latos-Grażyński, L. *Tetrahedron Lett.* **1999**, *40*, 8457.
(45) Stępień, M.; Latos-Grażyński, L. *Chem.*—Eur. J. **2001**, *7*, 5113.
(46) Jakobsen, H. J.; Ellis, P. D.; Inners, R. R.; Jensen, C. F. *J. Am. Chem. Soc.* **1982**, *104*, 7442.

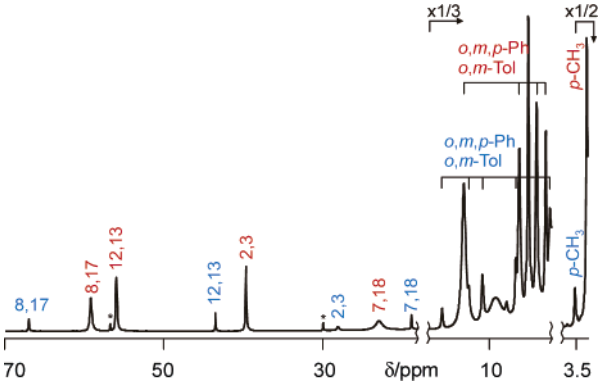

Figure 2. ^{1}H NMR spectra of **1**-NiCl ($CDCl_3$, 298 K). Resonance labeling: **1**-NiCl-o in red; **1**−NiCl-i in blue. Resonances of the nickel(II) 21-oxaporphyrin admixture are marked with an asterisk.

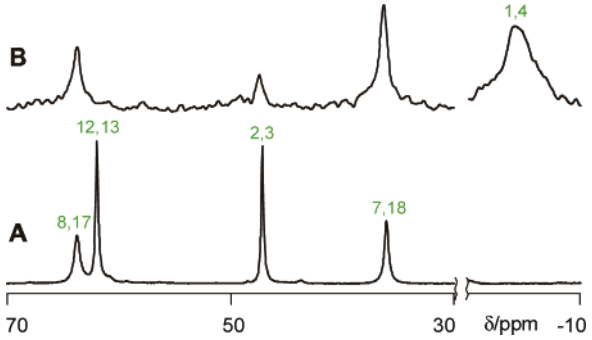

Figure 3. NMR spectra of (A) **1**-Ni$(CD_3OD)_2^+$ (^{1}H NMR, CD_3OD) and (B) partially deuterated **1**-Ni$(CH_3OH)_2^+$ (^{2}H NMR, CH_3OH, 298 K).

of two sets of resonances to **1**-NiCl-o and **1**-NiCl-i, respectively, has been based on a notion that a butadiene fragment in the folded conformation of **1**-NiCl-i blocks a coordination of the second axial ligand as discussed below which remains in contrast with the behavior of **1**-NiCl-o.

Relative amounts of the two isomers were estimated by careful deconvolution of the downfield region of the spectrum. Although the relative concentrations vary from synthesis to synthesis, the isomer **1**-NiCl-o is typically more abundant. This is a very important piece of information because of its analytical applications. Comparison of the relative intensities allows the selection of two sets of resonances, which belong to the two stereoisomers shown in Chart 6. The internal consistency of the integrated intensities for each set has been carefully checked. Resonances that belong to one isomer have a set of relative intensities that reflect the molecular structure. However, the intensities ratios between resonances that belong to different isomers reflect the relative populations of those isomers.

The ^{1}H NMR spectra of **1**-NiCl-o and **1**-NiCl-i shown in Figure 2 correspond to effective C_s symmetry of these molecules. The observed pattern of chemical shifts is quite typical for high-spin nickel(II) complexes of porphyrin analogues,[11] with the β-pyrrole resonances in the downfield region of 60 to 10 ppm and the *meso*-aryl peaks in the 0−10 ppm range. ^{1}H and ^{2}H NMR spectra for **1**-NiCl-o and **1**-NiCl-i and their transformation products are presented in Figures 2−6. The spectral parameters have been gathered in Table 2. Resonance assignments, which are given above

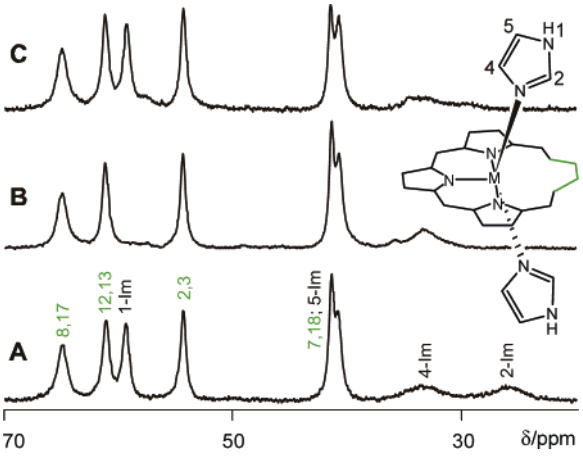

Figure 4. ^{1}H NMR ($CDCl_3$, 298 K) spectra of **1**-NiCl solution in the presence of (A) imidazole, (B) imidazole-1,2-d_2, and (C) imidazole-2,4,5-d_3. The labeling of imidazole resonances follows their position in the ring. The molar ratio **1**-NiCl:imidazole = 1:2.5.

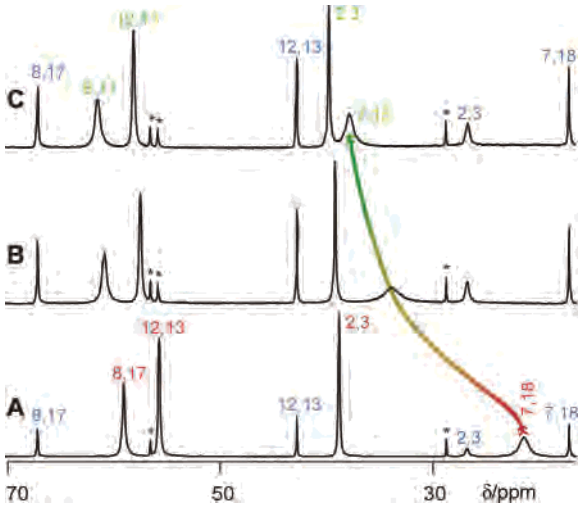

Figure 5. ^{1}H NMR titration of **1**-NiCl with benzyltriphenylphosphonium chloride ($CDCl_3$, 298 K). Number of equivalents added: (A) 0; (B) 1; (C) 5. Assignments are as in Figure 2, with the species **1**-$NiCl_2^-$ labeled in green. The nickel(II) 21-oxaporphyrin admixture is marked with an asterisk.

selected peaks, have been made on the basis of relative intensities, line widths, and site specific deuteration. The specific deuteration of vacataporphyrin, described above, allowed the detailed assignments of β-H resonances. As the spectroscopic analysis is primarily based on patterns of pyrrole resonances, the ^{2}H NMR spectra of nickel(II) vacataporphyrin is shown in Figure 3. The plots of the temperature dependence of the chemical shifts, which are typical for given electronic state of nickel vacataporphyrin, are shown in the Supporting Information (Figures 3S−5S).

Of special interest, however, are the shifts of the butadiene protons (Table 2). Signals 2,3-H of **1**-NiCl-o or **1**-NiCl-i present the chemical shifts typical for β-H pyrrolic positions of nickel(II) 21-heteroporphyrins despite the vacancy.[11] The extremely broad 1,4-H signal of **1**-NiCl-o has been detected by ^{2}H NMR spectroscopy at −3.5 ppm (298 K). The analogous resonance of **1**-NiCl-i has not been identified. The significant broadening of the 1,4-H signal relative to pyrrolic β-H, is caused by the proximity of the paramagnetic Ni(II) center.[47,48]

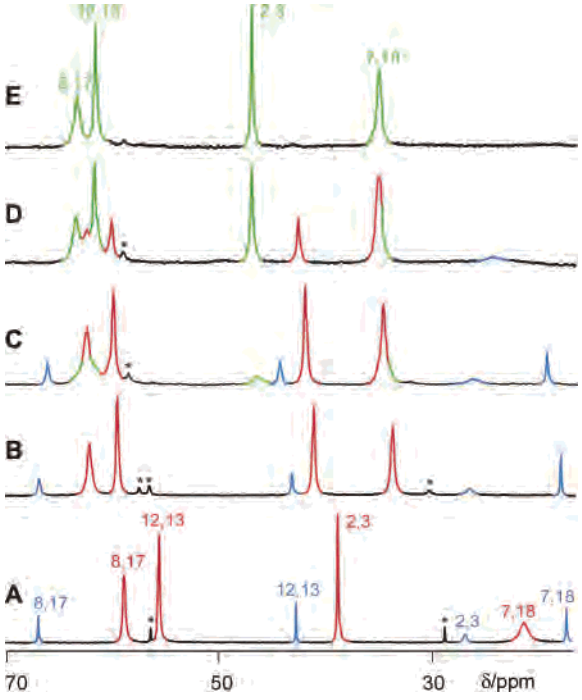

Figure 6. ^{1}H NMR titration of **1**-NiCl with methanol-d_4 ($CDCl_3$, 298 K). Amount of methanol added: (A) 0 equiv; (B) 5 equiv; (C) 6.3% v/v; (D) 15.1% v/v; (E) 25% v/v. Resonance assignments: **1**-NiCl-o in red; **1**-NiCl-i in blue; **1**-Ni$(CD_3OD)_2^+$ in green. The nickel(II) 21-oxaporphyrin admixture is marked with an asterisk.

Logarithms of $\nu_{1/2}$ plotted against T^{-1} yield linear plots (Supporting Information, Figures 1S and 2S) for **1**-NiCl-i suggest absence of any chemical exchange.[9,49,50] As expected, the slopes are positive and approximately equal for all protons in the molecule. It is essential to add that basically linear dependencies of log $\nu_{1/2}$ vs T^{-1} were previously observed for several paramagnetic nickel(II) heteroporphyrins and carbaporphyrins.[11,43,51−54]

On the other hand, the line widths of certain signals of **1**-NiCl-o exhibit an unusual temperature dependence characteristic of a dynamic process.[9,49,50] This behavior can be interpreted in terms of an conformational equilibrium in which one of the forms is present at a very small concentration and cannot be observed directly.[48,49,55] The conformational equilibrium presented at Scheme 1 may contribute to this mechanism providing that [**1**-NiCl-o] ≫ [**1**-NiCl-a] and the process is in the limit of slow exchange.

Thus in the same solution, two coexisting stereoisomers **1**-NiCl-o and **1**-NiCl-i reveal a different conformational flexibility. It is essential to notice here that the peculiar broadening of **1**-NiCl-o resonances is not related to relaxation effects but has its source in the dynamic properties of the vacataporphyrin ligand.

Nickel(II) Vacataporphyrin Containing Two Axial Ligands. The markedly different spectra of **1**-NiCl in methanol-d_4 (Figure 3) or acetonitrile-d_3 as compared to chlorinated solvents are attributed to an axial coordination of two solvent molecules with formation of a single species, i.e., **1**-Ni$(CD_3OD)_2^+$ or **1**-Ni$(CD_3CN)_2^+$, respectively, as shown in Chart 7.

Actually the axial bis-coordination produces the rather modest changes of the chemical shifts with one but very important diagnostic exception. Namely, the 7,18-H resonance undergoes the downfield relocation of ca. 20 ppm (298 K). This results in a unique spectroscopic pattern being an unambiguous evidence of bis-axial coordination (Table 2).

Such thesis has been confirmed by the ^{1}H NMR spectrum of the species where the axial ligand resonances could be directly observed. Thus, an addition of 2 equiv of imidazole converts **1**-NiCl-o and **1**-NiCl-i into **1**-Ni$(Im)_2^+$ (Figure 4). All resonances of the coordinated imidazole are clearly discernible and have been assigned by line width analysis and selective deuteration. Their position resembles one determined for other imidazole adducts of nickel(II) heteroporphyrins.[56]

Their integrated intensities indicate that two symmetry-equivalent imidazole ligands are bound. This observation along with the fact that overall pattern of the vacataporphyrin resonances of **1**-Ni$(CD_3OD)_2^+$ and **1**-Ni$(CD_3CN)_2^+$ appears to be retained in the spectrum of the imidazole adducts indicates that imidazole occupies two axial positions and rendering two sides of vacataporphyrin equivalent allows solely the "outward" macrocyclic conformation.

The titration of **1**-NiCl with [$BzPh_3P$]Cl (benzyltriphenylphosphonium chloride) reveals that two isomeric forms have a different affinity to the second chloride ligand. Understanding of this process is of particular importance considering the impact of the macrocyclic geometry on the overall properties of particular isomers. The effect of the chloride addition can be seen by comparing trace A of Figure 5 with traces B and C showing spectra of the sample with 0.5 and 5 equiv of the titrant added. The coordination of the second chloride results in the smooth downfield relocation of 7,18-H resonance accompanied by modest changes for other resonances assigned originally to **1**-NiCl-o (Figure 5, trace B). Actually the final spectrum reproduces those measured for **1**-Ni$(CD_3OD)_2^+$ and **1**-$(CD_3CN)_2^+$. Thus, the detected transformation is readily ascribed to the formation of **1**-$NiCl_2^-$, which remains in the fast exchange with **1**-NiCl-o. Contrary to **1**-NiCl-o, the positions of **1**-NiCl-i resonances remain constant through all titration. Thus, the spectroscopic evidence is consistent with the geometric constrains imposed

(47) La Mar, G. N.; Walker, F. A. NMR of Paramagnetic Porphyrins. In *The Porphyrins*; Dolphin, D., Ed.; Academic Press: New York, 1979; pp 57−161.
(48) Bertini, I.; Luchinat, C. *Coord. Chem. Rev.* **1996**, *150*, 1.
(49) Satterlee, J. D.; La Mar, G. N.; Bold, T. J. *J. Am. Chem. Soc.* **1977**, *99*, 1088.
(50) La Mar, G. N.; Sherman, E. O. *J. Am. Chem. Soc.* **1970**, *92*, 2691.
(51) Latos-Grażyński, L. *Inorg. Chem.* **1985**, *24*, 1681.
(52) Lisowski, J.; Latos-Grażyński, L.; Szterenberg, L. *Inorg. Chem.* **1992**, *31*, 1933.
(53) Chmielewski, P. J.; Latos-Grażyński, L.; Olmstead, M. M.; Balch, A. L. *Chem.*—Eur. J. **1997**, *3*, 268.
(54) Chmielewski, P. J.; Latos-Grażyński, L. *Inorg. Chem.* **1998**, *37*, 4179.
(55) Swift, T. J. The Paramagnetic Line width. In *NMR of Paramagnetic Molecules. Principles and Applications*; La Mar, G. N., Horrocks, W. D., Jr., Holm, R. H., Eds.; Academic Press: New York, 1973; pp 53−83.
(56) Latos-Grażyński, L.; Pacholska, E.; Chmielewski, P. J.; Olmstead, M. M.; Balch, A. L. *Inorg. Chem.* **1996**, *35*, 566.

Table 2. ^{1}H NMR Data for Nickel(II) Complexes of **1**

compd	1,4-butadiene	2,3-butadiene	8,17-pyrrole	7,18-pyrrole	12,13-pyrrole
1-NiCl-o	−3.5[a]	39.3	58.3	15.8	55.1
1-NiCl-i		27.8	67.1	18.5	43.4
1-$NiCl_2^-$	−3.3[a]	40.8	61.8	39.3	58.5
1-NiCl(MeOD)		43.1	62.6	35.8	60.3
1-$Ni(MeOD)_2^+$	−4.1[a]	47.4	63.4	35.8	61.8
1-$NiIm_2^+$		54.4	65.0	40.8	61.2

[a] Detected only in ^{2}H NMR.

Scheme 1. Conformational Equilibrium Involving the **1**-MCl Extended Isomers

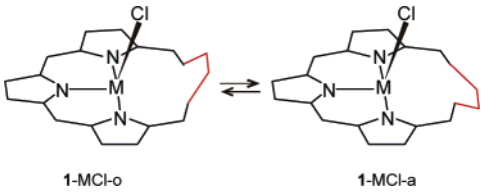

1-MCl-o **1**-MCl-a

Chart 7. Complexes Containing Two Axial Ligands

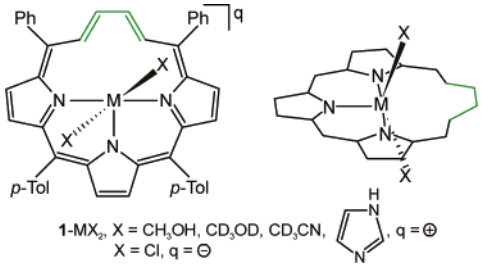

1-MX_2, X = CH_3OH, CD_3OD, CD_3CN, X = Cl, q = ⊖ , q = ⊕

by the **1**-NiCl-i structure. The butadiene fragment adjacent to the nickel(II) ion blocks sterically the coordination in the trans position to originally coordinated apical chloride.

The more complex behavior has been observed for the systematic titration of **1**-NiCl with CD_3OD (Figure 6). Initially, **1**-NiCl-o coordinates one molecule of methanol to form **1**-NiCl$(CD_3OD)^+$ which is in the fast exchange with **1**-NiCl-o. At this concentration of alcohol (5 equiv) **1**-NiCl-i is not involved in the process. Similarly as for the chloride titration, the geometry around **1**-NiCl-i prevents the coordination of the second axial ligand. The further changes in coordination sphere are forced by the large excess (25% v/v) of alcohol ligand yielding eventually **1**-$(CD_3OD)_2^+$ (Figure 6, trace E).

DFT Calculations. The strictly planar conformation of **1**-o has been observed in the solid state and in solution.[1] In analogy to an unorthodox geometry of 21,23-ditelluraporphyrin **6**,[23] the inverted geometry of the free ligand **1**-i has been suggested as well. Both geometries of **1** were subjected to a DFT optimization at the B3LYP/6-31G** level of theory (Supporting Information figures). In each case a genuine energy minimum was obtained. The calculated total energies, using the B3LYP/6-31G**//B3LYP/6-31G** approach (Table 3), demonstrate the planar conformer is more stable as shown by the DFT studies as the energy difference between **1**-o and **1**-i equals 8.6 kcal/mol. This energy difference accounts for the preference for **1**-o in the solution and in the solid state.

As shown above, the vacataporphyrin **1**-MCl complexes acquire preferentially two extreme conformations in solution. The existence of the third one has been inferred from the line width analysis. Thus, the conformational features of **1**-o are preserved after coordination in **1**-MCl-o and **1**-MCl-a. The butadiene unit is tilted away from the metal center with the C(2)−C(3) bonds and the axial MX bond in *syn* **1**-MCl-o or *anti* **1**-MCl-a orientations. (Scheme 1). The hypothetical unorthodox geometry **1**-i is trapped by coordination in **1**-MCl-i. This conformer locates the C(2)−C(3) bond in the coordination core in an *anti* orientation with respect to the axial MX bond. The experimentally observed conformers of **1**-MCl raised the question of their relative stability. To approach this problem we have applied the density functional theory (DFT) in a way similar to that previously described for metallobenziporphyrins.[8,9]

Using molecular mechanics and semiempirical calculations, we selected three principal geometries of **1**-CdCl, which were subjected to a DFT optimization at the B3LYP/LANL2DZ level of theory. The final geometries, **1**-CdCl-o, **1**-CdCl-i, **1**-CdCl-a, and **1**-$CdCl_2^-$, are shown in Figure 7. In each case a genuine energy minimum was obtained (B3LYP/LANL2DZ). The optimized structural parameters are contained in the Supporting Information (Figure 6S). Selected geometrical parameters and relative energies for **1**-CdCl are given in Table 3.

The angle between the butadiene plane and the plane of the three pyrrolic nitrogens (C_4/N_3) (Table 3) affects the M···C and M···H distances in the coordination core. For the sake of comparison, we bring to your attention that the angle between the *p*-phenylene plane and the plane of the three pyrrolic nitrogens (C_6/N_3) equals 52° as determined by X-ray studies for *para*-benziporphyrin to be reproduced by DFT calculations where the C_6/N_3 angle becomes 48°.[8]

The interaction, as quantified by the distances M···H and M···C (Table 3), is indeed affected by the conformational changes under study. For instance, in the **1**-CdCl-o conformer the calculated Cd···H(1) and Cd···H(2) distances equal 2.74 and 5.11 Å, respectively. The *anti* conformation changes the geometric factors, which is reflected in the spectroscopic data.

The energy ordering of the conformers in the **1**-CdCl series is **1**-CdCl-o < **1**-CdCl-i < **1**-CdCl-a. The small energy difference between **1**-CdCl-o and **1**-CdCl-i (2.3 kcal/mol) or **1**-CdCl-o and **1**-CdCl-a (6.6 kcal/mol) accounts for their simultaneous presence.

The bond distances within the tripyrrolic framework of complexes (Supporting Information, Figure 6S) indicate that this part of the macrocycle is highly conjugated in a similar manner for all forms. Similarly, the free ligand bond lengths have been preserved in two extreme conformations **1**-o and **1**-i.

Table 3. Selected DFT Data for **1**, **1**-CdCl, and **1**-$CdCl_2^-$

compd	energy (kcal)	Cd···Cl (Å)	Cd···C2 (Å)	Cd···H1 (Å)	Cd···H2 (Å)	C4/N_3[c] (°)
1-o	0[a]					2.4
1-i	8.6[a]					41.1
1-CdCl-o	0[b]	3.40	4.20	2.74	5.11	10.3
1-CdCl-i	2.3[b]	3.46	2.97	4.14	3.19	45.2
1-CdCl-a	6.6[b]	3.34	4.26	2.41	5.27	17.4
1-$CdCl_2^-$		3.13	3.91	2.49	4.84	18.4

[a] Compared to **1**-o. [b] Compared to **1**-CdCl-o. [c] The angle between the butadiene plane and the plane of the three pyrrolic nitrogens.

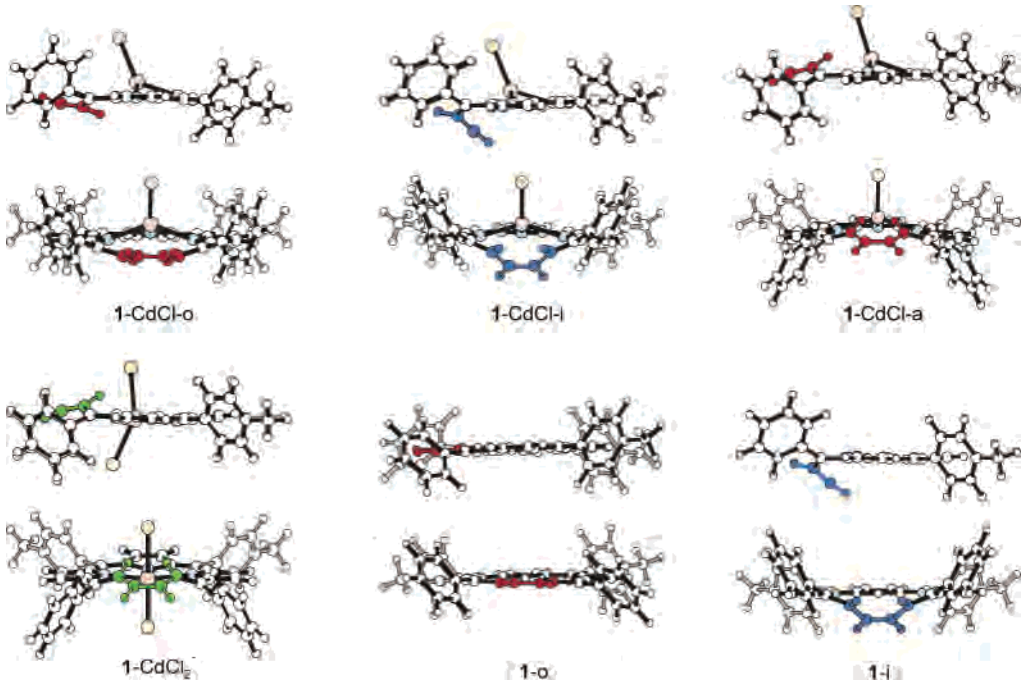

Figure 7. Geometries of **1** and the cadmium complexes of **1** obtained in a DFT optimization (B3LYP/LANL2DZ for the metal complexes; B3LYP/6-31G** for the free ligands). Projections emphasize the conformations of the macrocycle. The butadiene fragment is shown in red for "i" conformers, in blue for "o" conformers, and in green for **1**-$CdCl_2^-$.

Conclusions

Vacataporphyrin, which clearly belongs to the family of core-modified porphyrins and resembles the parent 5,10,-15,20-tetraarylporphyrin, reveals interesting properties as a ligand. The molecule coordinates via three nitrogen atoms. Due to coordination the macrocycle acquires two fundamentally different conformations affording, eventually, different modes of weak interaction between the central metal ion and the butadiene fragment. The macrocyclic conformation has been found to be instrumental in determination of coordinating properties in axial positions. A unique conformational flexibility of vacataporphyrin can be considered as a promising factor to be explored and applied in control of metalloporphyrinoid properties.

Experimental Section

Solvents and Reagents. Dichloromethane-d_2 and methanol-d_4 (CIL) were used as received. Chloroform-*d* (CIL) was passed through basic Al_2O_3. Imidazole-1,2-d_2 and imidazole-2,4,5-d_3 were prepared according to reported methods.[57]

Improved Synthesis of 1.[1] Solution of 60 mg (0.079 mmol) of 5,20-diphenyl-10,15-bis(*p*-tolyl)-21-telluraporphyrin, **2**,[38] in 30 mL of deoxygenated *o*-dichlorobenzene was placed in a 50 mL flask equipped with a reflux condenser. Nitrogen was bubbled very slowly through the solution, and 15 mL of 20% HCl was added dropwise to the refluxing solution during 1 h 30 min. The solvents were evaporated, and the residue was extracted with CH_2Cl_2 and chromatographed on basic alumina column. The first, minor fraction, eluted with CH_2Cl_2 contained unreacted 21-telluraporphyrin. The peach-red major product **1** was eluted as the second (after **2**) fraction. It was recrystallized from $CHCl_3$ with CH_3OH. Yield: 36 mg (0.057 mmol), 72%.

1-NiCl. A 10 mg (0.016 mmol) amount of **1** and 4.2 mg (0.032 mmol) of $NiCl_2$ were dissolved in an oxygen-free mixture of $CHCl_3$ (10 mL) and CH_3CN (15 mL). One drop of triethylamine was added, and the solution was refluxed under nitrogen for 2 h. The solvents were evaporated, and the residue was mixed with 10 mL of CH_2Cl_2 and filtered. After evaporation of the solvent the complex was recrystallized from CH_2Cl_2 and hexane. Yield: 95%. UV−vis (CH_2Cl_2, λ): 382 (sh), 435; 467 (sh); 547 (sh); 620; 651. ^{1}H NMR ($CDCl_3$, 298 K) for **1**-NiCl-o: δ 58.27 (s, 2H, 8,17); 55.06 (s, 2H, 12,13); 39.33 (s, 2H, 2,3); 35.8−15.8 (s, 2H, 7,18); 11.15, 8.77, 8.42, 8.10, 7.68 (18H, *o*-,*m*-,*p*-Ph; *o*-,*m*-Tol); 3.04 (s, 6H, *p*-Tol (CH_3)); −3.5 (br, s, 2H, 1,4). ^{1}H NMR ($CDCl_3$, 298 K) for **1**-NiCl-i: 67.06 (s, 2H, 8,17); 43.43 (s, 2H, 12,13); 27.8 (s, 2H, 2,3); 18.52 (s, 2H, 7,18); 11.9, 10.88, 10.32, 8.95, 7.74, 7.53 (18H, *o*-,*m*-,*p*-Ph; *o*-,*m*-Tol); 3.53 (s, 6H, *p*-Tol (CH_3)); (H-1,4 not visible). MS: m/z_{calc} for $NiC_{46}H_{34}N_3^+$ = 686.2106, m/z_{exp} = 686.2100.

(57) Vaugh, J. D.; Mugharbi, Z.; Wu, E. C. *J. Org. Chem.* **1970**, *31*, 1141.

1-CdCl. A 5.8 mg (0.032 mmol) amount of $CdCl_2$ was added to CH_3CN (10 mL) and refluxed with vigorous stirring for 15 min. A 10 mg (0.016 mmol) amount of **1** was dissolved in $CHCl_3$ (10 mL) with one drop of triethylamine and poured into the first solution. The color changes immediately from red to bright green. The mixture was refluxed for 20 min (UV−vis control). The solvents were evaporated, and the residue was mixed with 10 mL of CH_2Cl_2, filtered, and evaporated. Yield: 100%. UV−vis (CH_2Cl_2, λ): 439; 461 (sh); 623; 645; 695. ^{1}H NMR (CD_2Cl_2, 298 K) for **1**-CdCl-o: δ 9.27 (AA′XX′, 2H, 2,3); 8.37 (d, 2H, 8,17, $^4J_{H-Cd} = 4.2$ Hz); 8.13 (d, 2H, 7,18, $^4J_{H-Cd} = 4.5$ Hz); 8.00 (s, 2H, 12,13, $^4J_{H-Cd} = 6.5$ Hz); 7.84 (d, 4H, *o*-Ph); 7.98, 7.70 (2d, 4H, *o*-Tol); 7.62 (t, 4H, *m*-Ph); 7.55 (t, 2H, *p*-Ph); 7.47, 7.41 (2d, 4H, *m*-Tol); 2.58 (s, 6H, *p*-Tol (CH_3)); −1.50 (AA′XX′, 2H, 1,4, $J_{H-Cd} \approx 3$ Hz). ^{1}H NMR (CD_2Cl_2, 298 K) for **1**-CdCl-i: δ 7.57 (AA′XX′, 2H, 1,4, $J_{H-Cd} \approx 7$ Hz); 7.38 (d, 4H, *o*-Tol); 7.37 (d, 4H, *o*-Ph); 7.35−7.29 (m, 10H, *m*-Tol, *m*-Ph, *p*-Ph); 7.23 (d, 2H, 8,17, $^4J_{H-Cd} = 4.8$ Hz); 6.94 (d, 2H, 7,18, $^4J_{H-Cd} = 4.6$ Hz); 6.82 (s, 2H, 12,13, $^4J_{H-Cd} = 5.9$ Hz); 4.88 (AA′XX′, 2H, 2,3, $J_{H-Cd} \approx 8$ Hz); 2.44 (s, 6H, *p*-Tol (CH_3)). ^{13}C NMR: δ 165.4 (9,16-i), 162.2 (9,16-o), 150.9 (11,14-i), 150.4 (11,14-o), 148.7 (6,19-i), 147.1 (6,19-o), 143.9 (1,4-i), 142.2, 139.4 (5,10-i), 138.2 (8,17-o; 5,10-o), 138.0, 137.8 (*p*-Tol-i), 137.5 (*p*-Tol-o), 137.4 (8,17-i), 137.3 (C_1-Ph-o), 136.6 (2,3-i), 136.4 (C_1-Tol-i), 135.9, 135.6 (2,3-o), 132.5 (*o*-Ph-o), 131.0 (*o*-Ph-i), 130.8 (12,13-o), 130.6 (Ar-i), 129.9 (12,13-i), 129.6 (Ar-i), 127.7 (*m*-Ph-o), 127.6 (*p*-Ph-o), 127.4 (Ar-i), 127.1 (*m*-Tol-i; 7,-18-o; 7,18-i; Ar-i), 126.7 (*m*-Tol-o), 126.0 (1,4-o), 20.4 (CH_3-*p*-Tol-o), 20 (CH_3-*p*-Tol-o). MS: m/z_{calc} for $^{114}CdC_{46}H_{34}N_3^+ = 742.1794$, $m/z_{exp} = 742.1772$.

1-ZnCl. A 10 mg (0.016 mmol) amount of **1** was dissolved in a mixture of 20 mL of $CHCl_3$, 2 mL of MeCN, and 1 drop of triethylamine. A 4.4 mg (0.032 mmol) amount of $ZnCl_2$ was added and stirred in room temperature for 3 min. The solvents were evaporated, and the residue was mixed with 10 mL of CH_2Cl_2, filtered, and evaporated. Yield: 100%. UV−vis (CH_2Cl_2, λ): 388, 434, 462 (sh), 603 (sh), 656, 709. ^{1}H NMR for **1**-ZnCl-o**:** δ 8.96 (AA′XX′, 2H, 2,3); 8.21 (d, 2H, 8,17); 7.92 (d, 2H, 7,18); 7.86 (s, 2H, 12,13); 7.72 (d, 4H, *o*-Ph); 7.95, 7.68 (2br d, 4H, *o*-Tol); 7.56−7.48 (*m*, *m*-Ph, *p*-Ph); 7.46, 7.40 (2br d, 4H, *m*-Tol); 2.60 (*s*, 6H, *p*-Tol (CH_3)); −0.32 (AA′XX′, 2H, 1,4). ^{1}H NMR for **1**-ZnCl-i: δ 7.53 (d, 2H, *o*-Tol); 7.34−7.27 (m, 16H, *o*-Ph, *m*-Ph, *o*-Tol, *m*-Tol); 7.22 (t, 2H, *p*-Ph); 7.07 (AA′XX′, 2H, 1,4); 6.99 (d, 2H, 8,17); 6.60 (s, 2H, 12,13); 6.59 (d, 2H, 7,18); 5.91 (AA′XX′, 2H, 2,3); 2.45 (s, 6H, *p*-Tol (CH_3)). ^{13}C NMR: δ 167.9, 163.7, 150.2, 149.6, 147.6, 147.0, 146.1, 142.8, 140.2, 139.1, 138.6, 138.0, 137.8, 137.5, 136.3, 135.7, 132.0, 131.5, 131.1, 130.5, 129.8, 129.2, 129.0, 128.7, 128.3, 128.2, 128.1, 127.9, 127.6, 21.5, 21.3. MS: m/z_{calc} for $ZnC_{46}H_{34}N_3^+ = 692.2044$, $m/z_{exp} = 692.2006$.

Theoretical Calculations. DFT calculations were performed with the GAUSSIAN03 program.[58] Geometry optimizations were carried out within unconstrained C_1 symmetry. Starting geometries were obtained using molecular mechanics and semiempirical calculations. Becke's three-parameter exchange functional[59] with the gradient-corrected correlation formula of Lee, Yang, and Parr (DFT-(B3LYP))[60] were used with the LANL2DZ basis set for metal complexes. For free bases, the B3LYP/6-31G** approach was applied.[61]

Acknowledgment. Financial support from the Ministry of Scientific Research and Information Technology (Grant 3 T09A 162 28) is kindly acknowledged. DFT calculations were preformed at the Supercomputer Centers in Wrocław and Poznań, Poland.

Supporting Information Available: Total electronic energies and coordinates for the DFT-optimized structures (a listing in the *XYZ* format), Curie plots of paramagnetic shifts, and temperature dependency of line widths. This material is available free of charge via the Internet at http://pubs.acs.org.

IC0511470

(58) Frisch, M. J.; Trucks, G. W.; Schlegel, H. B.; Scuseria, G. E.; Robb, M. A.; Cheeseman, J. R.; Montgomery, J. A., Jr.; Vreven, T.; Kudin, K. N.; Burant, J. C.; Millam, J. M.; Iyengar, S. S.; Tomasi, J.; Barone, V.; Mennucci, B.; Cossi, M.; Scalmani, G.; Rega, N.; Petersson, G. A.; Nakatsuji, H.; Hada, M.; Ehara, M.; Toyota, K.; Fukuda, R.; Hasegawa, J.; Ishida, M.; Nakajima, T.; Honda, Y.; Kitao, O.; Nakai, H.; Klene, M.; Li, X.; Knox, J. E.; Hratchian, H. P.; Cross, J. B.; Adamo, C.; Jaramillo, J.; Gomperts, R.; Stratmann, R. E.; Yazyev, O.; Austin, A. J.; Cammi, R.; Pomelli, C.; Ochterski, J. W.; Ayala, P. Y.; Morokuma, K.; Voth, G. A.; Salvador, P.; Dannenberg, J. J.; Zakrzewski, V. G.; Dapprich, S.; Daniels, A. D.; Strain, M. C.; Farkas, O.; Malick, D. K.; Rabuck, A. D.; Raghavachari, K.; Foresman, J. B.; Ortiz, J. V.; Cui, Q.; Baboul, A. G.; Clifford, S.; Cioslowski, J.; Stefanov, B. B.; Liu, G.; Liashenko, A.; Piskorz, P.; Komaromi, I.; Martin, R. L.; Fox, D. J.; Keith, T.; Al-Laham, M. A.; Peng, C. Y.; Nanayakkara, A.; Challacombe, M.; Gill, P. M. W.; Johnson, B.; Chen, W.; Wong, M. W.; Gonzalez, C.; Pople, J. A. *Gaussian 03*, revision C.01; Gaussian: Pittsburgh, PA, 2004.
(59) Becke, A. D. *Phys. Rev. A* **1988**, *38*, 3098.
(60) Lee, C.; Yang, W.; Parr, R. G. *Phys. Rev. B* **1988**, *37*, 785.
(61) Hay, P. J.; Wadt, W. R. *J. Chem. Phys.* **1985**, *82*, 270, 284, 299.